Net-b, a Ras-Insensitive Factor That Forms Ternary Complexes with Serum Response Factor on the Serum Response Element of the *fos* Promoter

ANTOINE GIOVANE, PETER SOBIESZCZUK,† ABDELKADER AYADI, SAUVEUR-MICHEL MAIRA,
AND BOHDAN WASYLYK*

Institut de Génétique et de Biologie Moléculaire et Cellulaire, CNRS, INSERM, ULP, 67404 Illkirch cedex, France

The Ras signalling pathway targets transcription factors such as the ternary complex factors that are recruited by the serum response factor to form complexes on the serum response element (SRE) of the *fos* promoter. We have identified a new ternary complex factor, Net-b. We report the features of the *net* gene and show that it produces several splice variants, *net-b* and *net-c*. *net-b* RNA and protein are expressed in a variety of tissues and cell lines. *net-c* RNA is expressed at low levels, and the protein was not detected, raising the possibility that it is a cryptic splice variant. We have studied the composition of ternary complexes that form on the SRE of the *fos* promoter with extracts from fibroblasts (NIH 3T3) cultured under various conditions and pre-B cells (70Z/3) before and after differentiation with lipopolysaccharide (LPS). The fibroblast complexes contain mainly Net-b followed by Sap1 and Elk1. Net-b complexes, as well as Sap1 and Elk1, are induced by epidermal growth factor (EGF) stimulation of cells cultured in low serum. Pre-B-cell complexes contain mainly Sap1, with less of Net-b and little of Elk1. There is little change upon LPS-induced differentiation compared to the increase with EGF in fibroblasts. We have also found that Net-b is a nuclear protein that constitutively represses transcription. Net-b is not activated by Ras signalling, in contrast to Net, Sap1a, and Elk1. We have previously reported that down-regulation of Net proteins with antisense RNA increases SRE activity. The increase in SRE activity is observed at low serum levels and is even greater after serum stimulation, showing that the SRE is under negative regulation by Net proteins and the level of repression increases during induction. Net-b, the predominant factor in ternary complexes in fibroblasts, may both keep the activity of the SRE low in the absence of strong inducing conditions and rapidly shut the activity off after stimulation.

Thirty percent of human cancers contain activated mutant Ras proteins (29). Ras controls a signalling network that includes several parallel cascades of mitogen-activated protein (MAP) kinases. These cascades are conserved through evolution from yeasts to humans. They lead to phosphorylation of cellular effectors, including transcription factors of the Ets family, that have been found to be Ras targets in mammals, insects, and worms (6, 50). The Ets family is composed of at least 20 factors that contain the characteristic Ets DNA binding domain (52). Within the family, the Ras targets include Ets-1, Ets-2, Net (also called Erp and SAP2), Elk1, Sap1a, ERM, PEA3, and ERF in mammals; Yan/Pok and Pointed P2 in *Drosophila melanogaster*; and Lin1 in *Caenorhabditis elegans* (1–4, 7, 15, 25, 26, 31–33, 35, 36, 39, 40, 44, 48, 54, 55).

Net, Sap1, and Elk1 have three related sequences, A to C (Fig. 1A). The A regions are Ets DNA binding domains, the B boxes mediate interactions with serum response factor (SRF), and the C elements activate transcription once they have been phosphorylated by MAP kinases (8, 10, 27, 39). Net also contains an autonomous inhibitory domain (NID) that probably adopts a helix-loop-helix structure (34). Net, Sap1, and Elk1 are called ternary complex factors (TCFs), since they are re-

cruited by SRF to form ternary complexes (TCs) on the serum response element of the c-*fos* promoter. SRF binds tightly to the CArG box of the SRE, whereas the TCFs cannot bind alone because of the low affinity of the *ets* motif (10, 27, 39). The SRE mediates responses to a large number of extracellular signals, including serum, growth factors, tetradecanoyl phorbol acetate, lipopolysaccharide (LPS), and UV irradiation (24, 53). In vivo the SRE is constitutively occupied by a complex that appears to be a dimer of SRF and a TCF (18, 30). Extracellular signals are thought to lead to both phosphorylation of the components of the complex and changes in the composition due to the exchange of TCFs (9, 21, 46, 56).

The SRE has become a paradigm for the understanding of how a large number of signals can target a response element on a promoter and generate a specific response (24). An important goal is to identify all of the factors that intervene in the response. We have identified a new TCF, Net-b, that is expressed in many mouse tissues. It has the properties of a constitutive repressor that is not activated by Ras. It appears to be a major constituent of ternary complexes in fibroblasts and may keep the activity of the *fos* promoter low in the absence of strong inducing conditions (12).

* Corresponding author. Mailing address: Institut de Génétique et de Biologie Moléculaire et Cellulaire, CNRS, INSERM, ULP, 1 Rue Laurent Fries, BP 163, 67404 Illkirch cedex, France. Phone: 33-388 65 34 11. Fax: 33-388 65 32 01 and 33-388 65 32 46. E-mail: boh@igbmc .u-strasbg.fr.

† Present address: Biochemistry and Molecular Genetics, Imperial College School of Medicine at St. Mary's, London W2 1PG, United Kingdom.

MATERIALS AND METHODS

RNA purification. Total RNA was extracted with the Trizol kit (Gibco BRL), treated with RQ1 RNase-free DNase (Promega) for 1 h at 37°C, and extracted with phenol saturated with 100 mM sodium acetate (pH 4) to remove all traces of genomic DNA.

Reverse transcription-PCR. Total RNA (1 µg) was incubated for one cycle of 5 min at 94°C in 50 µl containing 10 mM Tris-HCl (pH 8.3), 50 mM KCl, 1.5 mM MgCl$_2$, 0.001% gelatin, 200 mM deoxynucleoside triphosphates, and 500 ng of each oligonucleotide. After 5 min at 55°C, 2.5 U of *Taq* polymerase (Perkin-Elmer Cetus) and 2 U of avian myeloblastosis virus reverse transcriptase (Phar-

A

B

Net-b
```
  1 MESAITLWQF LLHLLLLDQKH EHLICWTSND GEFKLLKAEE VAKLWGLRKN KTNMNYDKLS RALRYYYDKN
 71 IIKKVIGQKF VYKFVSFPDI LKMDPHAVEI SRESLLLQDG DCKVSPEGRE VHRHGLSSLK SASRNEYLHS
141 GLYSSFTINS LENAPEAFKA IKETKLEEPC DDSPPVEEVR TV[IR]QKTQRL GNLCTPTVAL RHRHRLHRPQ
211 QPSPPLRIPH SSLLHRTDTK WTVSGLESAA AQHTLLEQP
```

Net-c
```
  1 MESAITLWQF LLHLLLLDQKH EHLICWTSND GEFKLLKAEE VAKLWGLRKN KTNMNYDKLS RALRYYYDKN
 71 IIKKVIGQKF VYKFVSFPDI LKMDPHAVEI SRESLLLQDG DCKVSPEGRE VHRHGLSSLK SASRNEYLHS
141 GLYSSFTINS LENAPEAFKA IKETKLEEPC DDSPPVEEVR TV[IR]HQVDCF WPRVRCCPAY TSGAALVRSP
211 HE
```
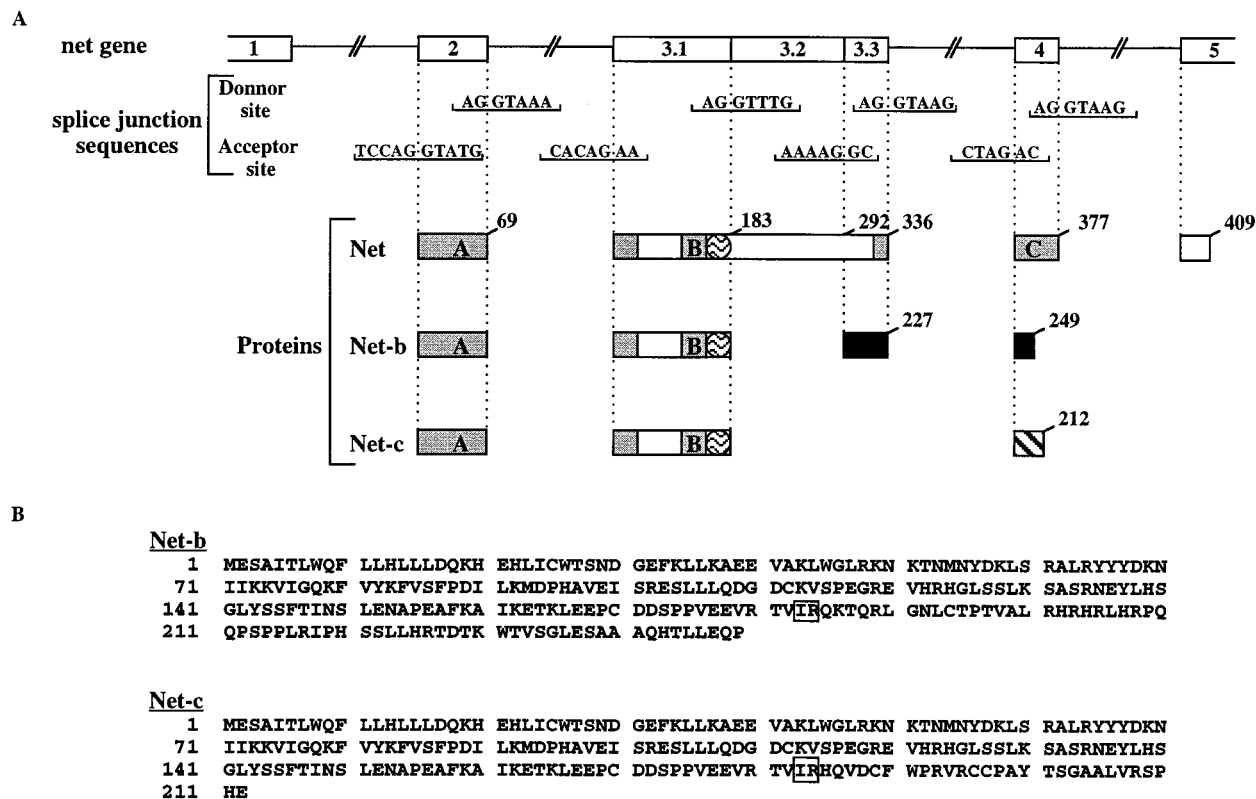
FIG. 1. Proteins encoded by the *net* gene. (A) The structure of the *net* gene, exon-intron junction sequences, and Net protein isoforms are illustrated. The numbers on the proteins indicate the amino acids at the splice junctions. Exons 3.2 and 3.3 for *net* are introns for *net-b* and *net-c*. A, B, and C in the Net protein indicate sequences that are conserved in other TCFs. The oval in Net shaded with wavy lines is the NID (34). Divergent sequences between Net, Net-b, and Net-c have different shadings. (B) Amino acid sequences of Net-b and Net-c. The boxed amino acids are at the junction between the common N-terminal and the divergent C-terminal sequences.

macia) were added and incubation was continued for 25 min at 55°C and 5 min at 94°C followed by 30 cycles of 30 s at 94°C, 30 s at 60°C, and 30 s at 72°C. Different pairs of oligonucleotides were used to analyze Net, Net-b, and Net-c expression. The PCR products were analyzed by electrophoresis on 5% poly-acrylamide gels, staining with ethidium bromide, and visualization under UV. Oligonucleotides 1 and 2 amplify *net-b* and *net-c* mRNA, 6 and 7 amplify *net*, 3 and 4 amplify *net-b*, 5 and 6 amplify *net-c*, and 8 and 9 amplify G6PD (glucose 6-phosphate dehydrogenase) mRNA. The PCR products were sequenced by the dideoxynucleotide chain termination method both manually and with an auto-matic sequencer (Applied Biosystems) to confirm their identity. The oligonucle-otides are as follows: 1, 5′ AATTCCCGGGCCCACACCAATGGAGAGTGCA ATCACGCTGTGG (Net, Net-b, Net-c); 2 5′ CCTAAGCTTTCATGACACAG GTAAACTAGC (Net, Net-b, Net-c); 3, 5′ GTCAGGACTGTGATCAGGCAA (Net-b); 4, 5′ GAGGCCAGAAACAGTCCACTTG (Net-b); 5, 5′ TCCACTTG GTGTCTGATCACA (Net-c); 6, 5′ AACTACGACAAGCTGAGGAGAGC (Net-c, Net); 7, 5′ AGCGGTCTCGGATGTGGAAGG (Net); 8, 5′ ATCTACC GCATTGACCACTACCTG (G6PD); and 9, 5′ CCCACAGAAGACATCCAG-GATGAG (G6PD).

Genomic structure. A mouse genomic library, constructed by inserting a par-tial *Sau*3A digest of ES cell DNA (D3 line from SV129 strain) in λ EMBL3 (*Bam*HI cloning site), was screened with full-length *net* cDNA. Fragments sub-cloned in pBluescript SK were restriction mapped and sequenced to establish the exon-intron boundaries.

Antibodies, Western blots, and nuclear extracts. Net, Net-b, Net-c, Sap1, and Elk1 antisera were raised in rabbits against the following ovalbumin-MBS-cou-pled peptides [200 mg/injection, cysteine (C) was added for coupling]: Ab n, 385-(C)HMPVPHPSLDRAPSPVLLSPSSQKS-409 (Net); Ab nbc, 157-(C)AF-KAIKTEKLEEPCDDSPPVEE-178 (Net, Net-b and Net-c); Ab b, 225-(C)HRT-DTKWTVSGLESAAAQHTLLEQ-249 (Net-b); Ab c, 196-(C)1CPAYTSGAA LVRSPHE-211 (Net-c); Ab sap, 109-(C)SIETSSSKDVEYGGKEYGGKERP PQPGAK-138 (Sap1); and Ab elk, 411-(C)SVDGLSTRVVLSPGPQK-427 (Elk1).

Nuclear extracts (100 to 200 μg of protein) were electrophoresed on sodium dodecyl sulfate–10% polyacrylamide gels, transferred to 0.2-μm-pore-size nitro-cellulose membranes, and detected with the serum antibodies and the enhanced chemiluminescence detection kit (Amersham). NIH 3T3 cells were serum starved for 48 h and treated with 50 ng of epidermal growth factor (EGF) per ml.

70Z/3 cells were incubated with 15 μg of LPS (serotype O128:B12; Sigma) per ml. Nuclear extracts were prepared by Nonidet P-40 lysis followed by high-salt extraction in the presence of protease and phosphatase inhibitors, as described by Sadowski and Gilman (42). Protein concentrations were determined by the Bradford assay.

Recombinants. pTL2-net-b and pTL2-net-c were constructed by inserting *Xma*I-*Hin*dIII fragments generated by RT-PCR with primers 1 and 2 (see above) in the corresponding sites of the pTL2 expression vector. pGFP.Net, pGFP.Net-b, and pGFP.Net-c were constructed by *Kpn*I-tagged PCR with, as templates, pTL2.Net, pTL2.Net-b, and pTL2.Net-c, respectively. The oligonu-cleotides used were as follows: 5′, CGG GGT ACC CCG ATG GAG AGT GCA ATC ACG CTG TG; and 3′, CGG GGT ACC TCA TCA GGA TTT CTG AGA GCT GGG GC. PCR fragments were clones in the KpnI site of pE.GFP.C1 vector (Clontech).

In vitro transcription and translation. pSG5-derived expression vectors were transcribed and translated in vitro in TnT rabbit reticulocyte lysates (Promega) with [^{35}S]methionine and analyzed by sodium dodecyl sulfate-polyacrylamide gel electrophoresis (10% polyacrylamide). The proteins were quantitated by scan-ning specific bands with a Fuji phosphorimager, taking into account the number of methionines.

Mobility shift assays. The assay mixtures contained either equimolar amounts of in vitro-translated proteins (adjusted to 5 μl with mock extracts that had been incubated without added expression vector) or 30 μg of nuclear extract proteins from NIH 3T3 or 70Z/3 cells. They were incubated for 60 min at 20°C in 20 μl of buffer [5 mM HEPES (pH 7.9), 2.5 mM MgCl$_2$, 2.5 mM EDTA, 2 mM spermidine, 2.5 mM dithiothreitol, 2 mg of bovine serum albumin per ml, and, as indicated in the figure legends, 1 μg of poly(dI-dC), 250 ng of salmon sperm DNA, and 20% glycerol or 4% Ficoll], plus 6 μl of antiserum (as indicated) and excess SRE probe. The samples were loaded on prerun [40 min at 30 mA [150 V]) 3.5% polyacrylamide gels (acrylamide-bisacrylamide ratio, 29:1) in 0.25 × Tris-borate-EDTA (TBE)–2.5% glycerol (where indicated in the figure legends) and run for 2 h at 30 mA (150 V) with recirculating buffer at 20°C. Bacterially expressed recombinant SRF core was prepared by the method of Hipskind et al. (21).

The oligonucleotides used for mobility shifts were as follows: SRE-WT, 5′-ACACAGGATGTCCATATTAGGACATCT; SRE-mut ets, 5′-ACACA ACTTGTCCATATTAGGACATCT; and SRE-mut SRF, 5′-ACACAGGATGT

CCATCGGCTGACATCT. The *ets* and SRF motifs are underlined. Only one strand of the double-stranded blunt-ended probes is shown. The oligonucleotides were 5′-end labelled with T4 polynucleotide kinase and purified on native 10% polyacrylamide gels.

Cell culture and transfections. The cells were maintained in Dulbecco's modified Eagle's medium (DMEM) with 10% fetal calf serum. NIH 3T3 cells were transfected by the calcium phosphate method with, per 100-mm dish, 20 μg of plasmid DNA containing expression vectors for the factors, 3 μg of pSG5-lacZ (control for the efficiency of transfection), 2.5 μg of reporters, and completed with pSG5. Cells that were 30% confluent were incubated with precipitated DNA for 24 h, washed three times with DMEM, incubated with DMEM plus 10% fetal calf serum for 24 h, scraped, subjected to three freeze-thaw cycles in solution A (15 mM Tris-HCl [pH 7.9], 60 mM KCl, 15 mM NaCl, 2 mM EDTA, 0.15 mM spermine, 1 mM dithiothreitol, 0.4 mM phenylmethylsulfonyl fluoride PMSF), and centrifuged. The transfection efficiency was corrected for β-galactosidase activity. Before the chloramphenicol acetyltransferase (CAT) assay, extracts were heated for 10 min at 65°C. Acetylated chloramphenicol was separated by thin-layer chromatography with 95% chloroform–5% methanol as the solvent, and the radioactivity was quantitated with a Fuji PhosphorImager. The experiments were repeated at least three times.

GFP cytofluorescence. NIH 3T3 cells were seeded in six-well cluster dishes (Costar) containing sterile coverslips and transfected with vectors that express green fluorescent protein (GFP) fusion proteins. After transfection (see above), the cells were washed three times with phosphate-buffered saline (PBS) and fixed with 4% paraformadehyde in PBS for 30 min. The coverslips were then removed from the wells, washed three times with PBS, and stained with Hoechst dye (5 μg/ml in PBS) to visualize the nuclei. After extensive washing in PBS, the coverslips were mounted on slides with one drop of mounting solution (50 g of propylgallate per liter in glycerol, 80%; PBS, 20%). The slides were examined under a fluorescence microscope.

RESULTS

Identification of the *net* splice variants *net-b* and *net-c* at the RNA level. During our initial isolation of *net* RNA from NIH 3T3 cells by RT-PCR with primers complementary to the start and stop codons (10), we cloned several shorter products that, upon sequencing, were found to have internal deletions of the net coding sequence. We further analyzed *net* RNA in NIH 3T3 cells by RT-PCR with three different pairs of primers. The PCR products were sequenced directly and found to have the same sequence as the original cloned fragments. Furthermore, *net-b* RNA was also detected by RNase mapping (results not shown). The *net-b* and *net-c* cDNAs have deletions of 325 and 455 bp compared to *net* (Fig. 1A). These variants of *net* could account for some of the different-sized *net* RNAs detected in mice (10, 33).

The *net* gene was analyzed for the presence of splice consensus sequences corresponding to the deletion endpoint. A lambda EMBL3 phage mouse genomic library was screened with the 2.6-kbp *net* cDNA probe (10), and clones containing at least five exons for *net* mRNA were isolated (Fig. 1A). Fragments containing exons 2 to 4 were subcloned, and the exon/intron boundaries were found to have sequences compatible with the consensus. The sequence deleted in *net-b* (exon 3.2) is entirely within exon 3 for *net* mRNA. However, there are consensus splice junction sequences in *net* coding sequences that correspond precisely to the expected AG-GT and AG-G sequences at the 5′ and 3′ boundaries, respectively, and there is a pyrimidine-rich region in exon 3 (45). The intronic sequences between exons 3 and 4 are spliced out in the same manner for *net* and *net-b*. Splicing in *net-c* removes exons 3.2 and 3.3. The 5′ splice junction is the same as for *net-b* mRNA, and the 3′ splice junction is in common with *net* and *net-b*. Only one *net* gene locus has been identified in a number of studies (11), indicating that *net*, *net-b*, and *net-c* mRNA are produced by alternative splicing, rather than transcription of several different genes with different structures.

Expression patterns of *net-b* and *net-c* mRNA. Expression of *net* RNA was assessed by RT-PCR analysis of total RNAs from various murine cell lines and tissues with primers specific for each mRNA (Fig. 2A). The *net* specific primers amplify se-
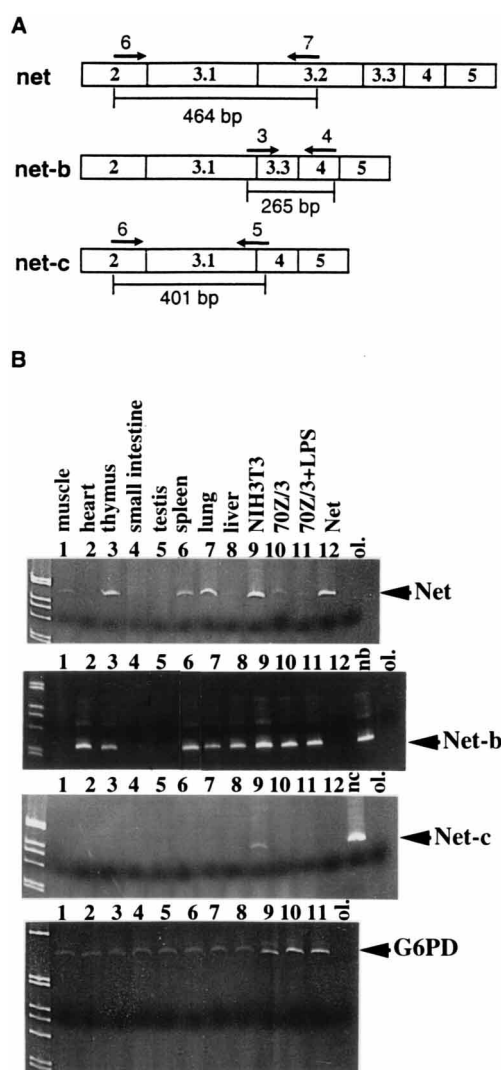

FIG. 2. Semiquantitative RT-PCR of *net*, *net-b*, *net-c*, and G6PD RNA. (A) Positions of the primers used for splice-variant specific PCR. The numbers indicate exons (Fig. 1A). (B) RT-PCR products were analyzed by electrophoresis on a 5% polyacrylamide gel and staining with ethidium bromide. The arrows indicate specific bands. RT-PCR mixtures contained 1 μg of total RNA from mouse skeletal muscle, heart, thymus, small intestine, testis, spleen, lung, liver, NIH 3T3, 70Z/3, 70Z/3 differentiated with LPS, oligonucleotides without RNA (ol.), and various in vitro transcribed RNAs: *net*, *net-b* (nb), and *net-c* (nc). The sizes of the marker bands in the three top panels are 517, 506, 396, 344, 298, 220, and 201 bp from top to bottom.

quences that are deleted in *net-b* and *net-c*. For both *net-b* and *net-c*, one of the primers overlaps the splice junction so that at stringent temperatures they are specific and do not amplify full-length *net* (Fig. 2B; see the controls with the specific primers [Net-b, second panel; Net-c, third panel] with in vitro synthesized RNAs [Net-b, lane nb, second panel; Net-c, lane nc, third panel; Net, lanes 12 in the top three panels]). *net* mRNA was detected predominantly in thymus, spleen, lung, and NIH 3T3 cells (Fig. 2B, lanes 3, 6, 7, and 9, 464-bp band); there were lower levels in muscle, small intestine, testis, liver, and 70Z/3 cells (lanes 1, 4, 5, 8, 10, and 11) and no detectable expression in heart tissue (lane 2). These results were obtained under limiting PCR conditions, such that increasing the numbers of cycles further increased the synthesis of the specific products. When the number of cycles was increased, *net*-specific products
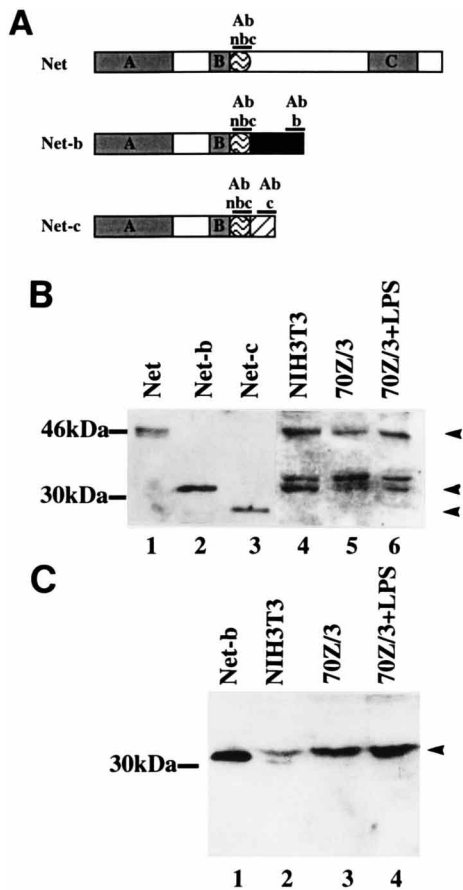
FIG. 3. Western blots of Net, Net-b, and Net-c. (A) Epitopes recognized by Ab nbc, Ab b, and Ab c. Ab nbc interacts with the NID present in Net, Net-b, and Net-c (circle with wavy lines), and Ab b and Ab c interact with sequences that are unique to Net-b and Net-c, respectively. (B and C) Western blots of extracts from COS cells transfected with the indicated expression vectors (B, lanes 1 to 3; C, lane 1), NIH 3T3 cells (100 μg) (B, lane 4; C, lane 2), 70Z/3 cells (200 μg) (B, lane 5; C, lane 3), and 70Z/3 cells stimulated with LPS (200 μg) (B, lane 6; C, lane 4). The membranes were probed with Ab nbc (B) or Ab b (C).

FIG. 4. Net-b and Net-c require SRF to bind to the SRE, similar to the other TCFs. Equal amounts of [^{35}S]methionine-labelled proteins synthesized in rabbit reticulocyte lysates (RL) were used. The band shift contained Net, Net-b, Net-c, Sap1a, Elk1, SRF, and core SRF (amino acids 132 to 222). The slanted arrowheads point to TCs, and the horizontal arrowheads point to binary complexes containing SRF (lanes 7 to 13) or core SRF (lanes 14 to 20). The incubation mixture included 20% glycerol, 1 μg of poly(dI-dC), and 250 ng of salmon sperm DNA, and the gels contained 2.5% glycerol.

were clearly detected in the samples with lower expression levels (not shown). *net-b* was detected in heart, thymus, spleen, lung, liver, NIH 3T3, and 70Z/3 and 70Z/3+ LPS cells (lanes 2, 3, 6, 7, 8, 9, 10, and 11; see the 265-bp *net-b* band). net-c was detected only in NIH 3T3 (lane 9; 401-bp band) and FR 3T3 (data not shown) cells. Control RT-PCRs for G6PD, a housekeeping gene, gave similar amounts of the specific product (750-bp product, bottom panel), showing that the differences were not due to quantitative variations in the amount of total RNA.

Net-b protein is expressed in the NIH 3T3 and 70Z/3 cell lines. The alternative splicing in *net-b* and *net-c* RNAs changes the reading frame. Net-b and Net-c are 249- and 212-amino-acid proteins, respectively, that have different C-terminal sequences from Net; in particular, they lack the C domain (Fig. 1B), the target for the Ras signalling pathway. In common with Net, they have the Ets domain, the B domain that interacts with SRF, and the helix-loop-helix motif of the Net inhibitory domain NID (amino acids 151 to 184). Expression of the variant proteins was studied with rabbit polyclonal antibodies raised against peptides (see Materials and Methods). Ab b and Ab c specifically recognize C-terminal sequences unique to Net-b and Net-c, respectively (Fig. 3A). Ab nbc has been described previously (PAb 376, [34]) and recognizes a sequence
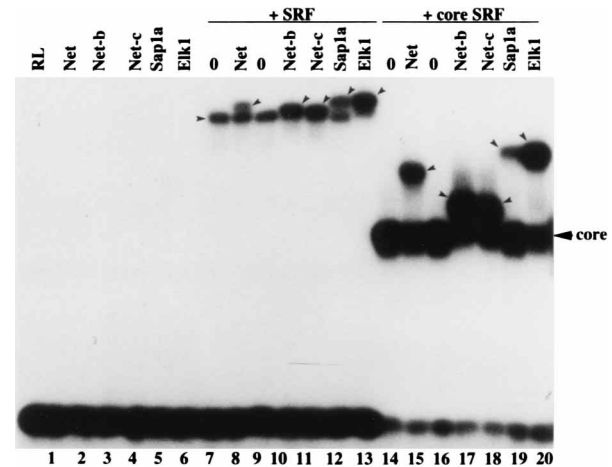
next to the B domain common to Net, Net-b, and Net-c. Extracts from NIH 3T3 and 70Z/3 cells (with or without LPS) and control transfected COS cells were used in Western blots. Ab nbc detected the expected 46-kDa band of exogenous Net in COS extracts and endogenous Net in NIH 3T3 and 70Z/3 extracts (Fig. 3B, lanes 1 and 4 to 6). It also revealed predicted 32- and 28-kDa proteins in Net-b- and Net-c-transfected COS extracts, respectively (lanes 2 and 3). The 32-kDa band was detected in NIH 3T3, 70Z/3, and 70Z/3+LPS extracts as the lower band of a doublet (lanes 4 to 6), whereas a 28-kDa protein was not detected. Ab b revealed uniquely the 32-kDa band in *net-b* transfected COS, NIH 3T3, 70Z/3, and 70Z/3+LPS extracts (Fig. 3C, lanes 1 to 4). Ab c did not detect a 28-kDa band in NIH 3T3, 70Z/3, or 70Z/3+LPS extracts (data not shown). These results show that NIH 3T3 and 70Z/3 cells express Net and Net-b proteins and that differentiation with LPS does not affect this expression. Net-c was not detected at the RNA level in most of the cell types tested or at the protein level in both Western blots and supershifts (see below) in NIH 3T3 cells, suggesting that it was expressed at most at low levels and/or in a very restricted manner.

Net, Net-b, and Net-c form TCs with SRF and the SRE in vitro. The capacity of Net-b and Net-c to form TCs was compared with that of Net, Sap1a, and Elk1. Equal amounts of in vitro-synthesized proteins were used in band shifts with the SRE DNA probe, either alone or in the presence of constant amounts of SRF or core SRF (Fig. 4). Like Net, Sap1a, and Elk1, Net-b and Net-c did not bind alone to the SRE (lanes 1 to 6) but did form complexes with the near-consensus PEA3* probe (data not shown). They formed retarded mobility complexes in the presence of SRF and core SRF (compare lanes 10 and 11 with lanes 7 and 9, and compare lanes 17 and 18 with lanes 14 and 16) with greater efficiently than Net or Sap1a (lanes 8, 12, 15, and 19) and as efficiently as Elk1 (lanes 13 and 20). These results show that Net-b and Net-c function as TCFs, as expected from the presence of the B domain.

Effects of stimuli of growth and differentiation on TC formation. EGF stimulates the growth of NIH 3T3 cells, and LPS induces the differentiation of 70Z/3 cells. Their effects on TC
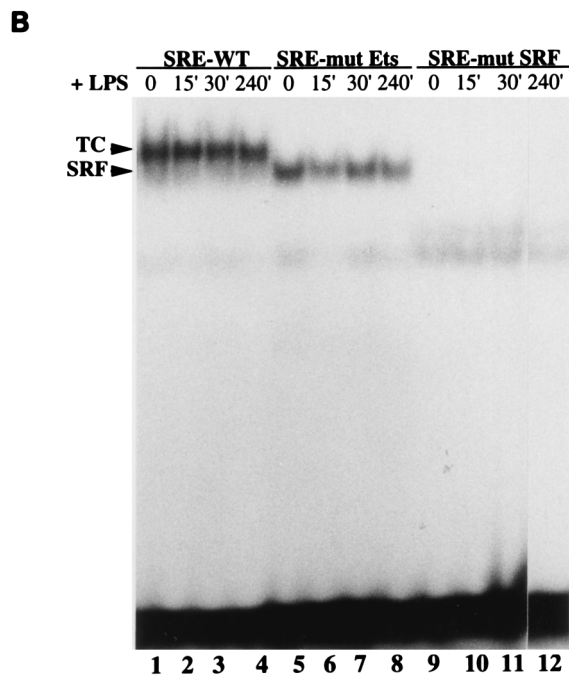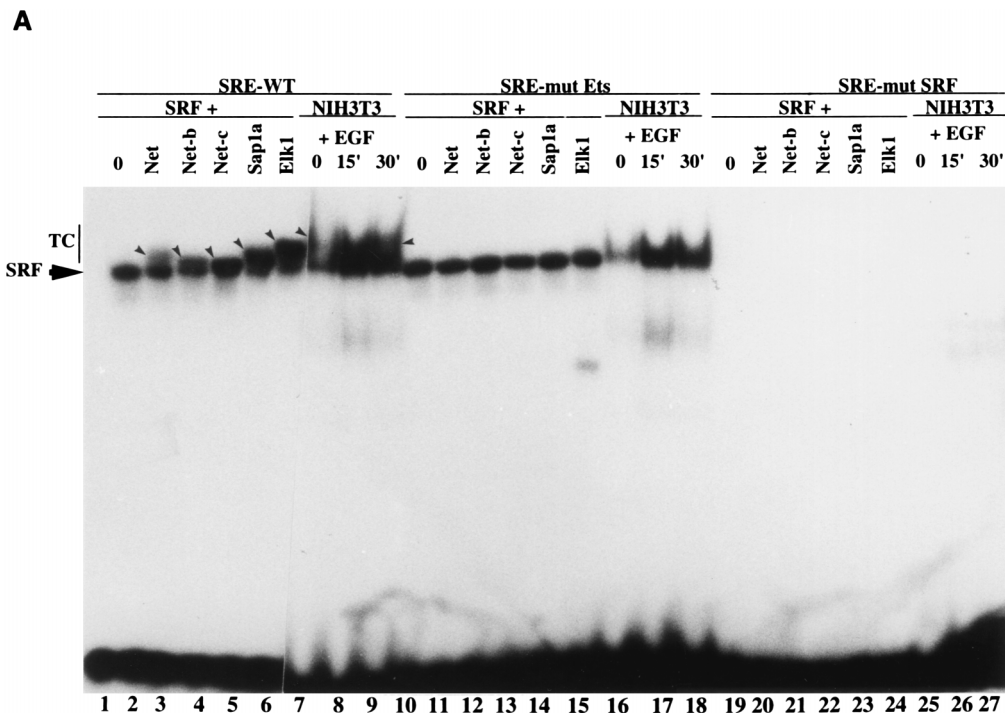
A

B

FIG. 5. TC formation by extracts from NIH 3T3 (A) and 70Z/3 (B) cells. The band shifts contained in vitro-synthesized proteins (A, lanes 1 to 6, 11 to 15, and 19 to 24) and nuclear extracts from NIH 3T3 cells (30 μg) (A, lanes 7 to 9, 16 to 18, 25 to 27) or 70Z/3 cells (B, lanes 1 to 12). The probes were SRE wild type (SRE-WT), SRE mutated in the *ets* site (SRE-mut Ets), and SRE mutated in the SRF site (SRE-mut SRF). The in vitro-synthesized proteins were SRF, Net, Net-b, Net-c, Sap1a, and Elk1. The NIH 3T3 cell extracts were serum starved (A, lanes 7, 16, and 25) or treated with EGF for 15 min (A, lanes 8, 17, and 26) or 30 min (A, lanes 9, 18, and 27). The 70Z/3 extracts were untreated (B, lanes 1, 5, and 9) or treated with LPS for 15 min (B, lanes 2, 6, and 10), 30 min (B, lanes 3, 7, and 11), or 240 min (lanes 4, 8, and 12). SRF, SRF complexed with the SRE. The incubation mixes included 20% glycerol, 1 μg of poly(dI-dC), and 250 ng of salmon sperm DNA, and the gels contained 2.5% glycerol.

formation were studied in cell extracts. Serum-starved NIH 3T3 extracts formed predominantly one major band and a smaller amount of lower-mobility complexes with the SRE probe (Fig. 5A, lane 7). The major band is probably an SRF-SRE complex, since it comigrated with the SRF-SRE complex formed with in vitro-translated proteins (lane 1) and was detected when the *ets* motif was mutated (lanes 16 and 10) but not when the SRF motif was altered (lanes 25 and 19). The lower-mobility bands correspond to TCs, since they comigrated with the in vitro complexes (lanes 2 to 6) and required intact *ets* and SRF motifs (compare lane 16 with lanes 11 to 15 and compare lane 25 with lanes 20 to 24). EGF stimulated the formation of both TCs (compare lanes 8 and 9 with lanes 17 and 18 and lanes 26 and 27) and SRF-SRE complexes (compare lanes 17 and 18 with lanes 26 and 27). In uninduced 70Z/3 cell extracts, the TCs were the major form (Fig. 5B, compare lanes 1, 5, and 9), and LPS did not affect complex formation (lanes 2 to 4, 6 to 8, and 10 to 12). These results show that the amount of TC formation increases upon stimulation of growth but not induction of differentiation. We used supershifts to study the components of the TCs.

Characterization of antibodies for supershifts. The antibodies were initially tested in in vitro experiments, to ascertain their specificity and effect on complex stability. The antibodies displayed their expected specificities (Fig. 6A), displacing the cognate TCs (Fig. 6B, compare the indicated lanes with the equivalents containing heterologous antibodies, and see Fig. 4). We found that (i) Ab n supershifted Net (lane 1); (ii) Ab nbc supershifted Net, Net-b, and Net-c (lanes 6 to 8); (iii) Ab b supershifted Net-b (lane 12); (iv) Ab c supershifted Net-c (lane 18); (v) Ab sap supershifted Sap1a (lane 24); (vi) Ab elk supershifted Elk1 (lane 30); and (vii) Ab srf, directed against the C terminus of SRF, supershifted all the TCs (lanes 31 to
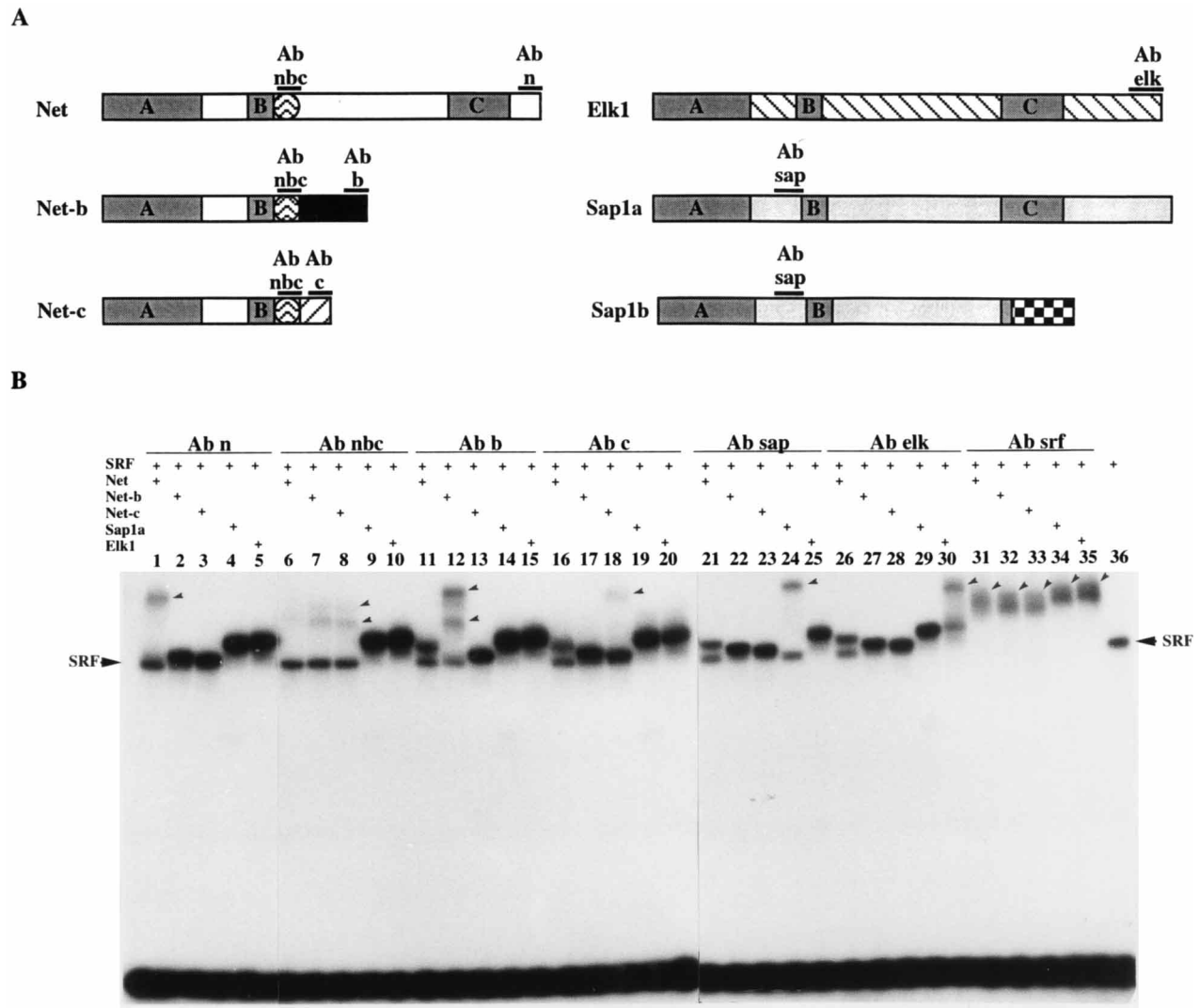
A

B

FIG. 6. Characterization of the antibodies used for supershift experiments. (A) Epitopes recognized by the antibodies. Ab nbc interacts with Net, Net-b, and Net-c; Ab n interacts with Net; Ab b interacts with Net-b; Ab c interacts with Net-c; AI elk interacts with Elk1; and Ab sap interacts with SAP1 (both isoforms). A, B, and C are related domains in the TCFs. (B) TCs formed between SRF and Net, Net-b, Net-c, Sap1a, and Elk1 were incubated with Ab n, Ab nbc, Ab b against Net-b, Ab c, Ab sap, Ab elk, or Ab srf against the C terminus of the SRF protein. The supershifted complexes are indicated by arrowheads. The incubation mixes included 20% glycerol, 1 μg of poly(dI-dC), and 250 ng of salmon sperm DNA, and the gels contained 2.5% glycerol.

35). All the antibodies completely shifted the TCs, except for Ab elk, which displaced about 50% (compare lanes 1, 6 to 8, 12, 18, 24, and 31 to 35 with lane 30). This was taken into account in the studies described below, by increasing the quantity of antibodies and controlling with in vitro-synthesized proteins. Ab n and Ab srf generated predominantly one major complex of similar intensity as the starting TC (lanes 1 and 31 to 36), whereas Ab c and Ab sap gave mainly one complex of lower intensity than the uncomplexed TC (lanes 18 and 24). Ab nbc and Ab b gave two major bands (lanes 6 to 8 and 12). Antibody binding to the TCFs was not sufficient to induce complex formation with the SRE in the absence of SRF (data not shown). This analysis suggests that the antibodies can be used to unambiguously identify the TCFs in the TCs. However, they have different effects on the complexes, and consequently the relative intensities of the supershifts for different factors are not a direct measure of their relative levels.

Composition of TCs under a variety of growth conditions and in different cell types. Initially, continuously growing NIH 3T3 cell extracts were tested in supershift experiments (Fig. 7), using both the consensus *ets* motif (PEA3*) and SRE probes. With the consensus *ets* probe, we detected a specific complex (Fig. 7A, lane 3) that comigrated with in vitro-synthesized Net-b (lane 1) and that was supershifted with antibodies that interact with Net-b (Ab nbc [lanes 7 and 9] and Ab b [lanes 10 and 12]) but not those that bind specifically to Net or Net c (Ab n [lanes 4 and 6] and Ab c [lanes 13 and 15]). A complex with the mobility of Net-c was not detected (lanes 2, 3, 5, 6, 8, 9, 11, 12, 14, and 15). The band that migrated more slowly and just above Net-b is not due to a TCF. It does not comigrate with Elk1 and Sap1 and is not displaced by any of our TCF antibodies (data not shown). These results demonstrate that Net-b can be detected in NIH 3T3 cell extracts by supershift exper-
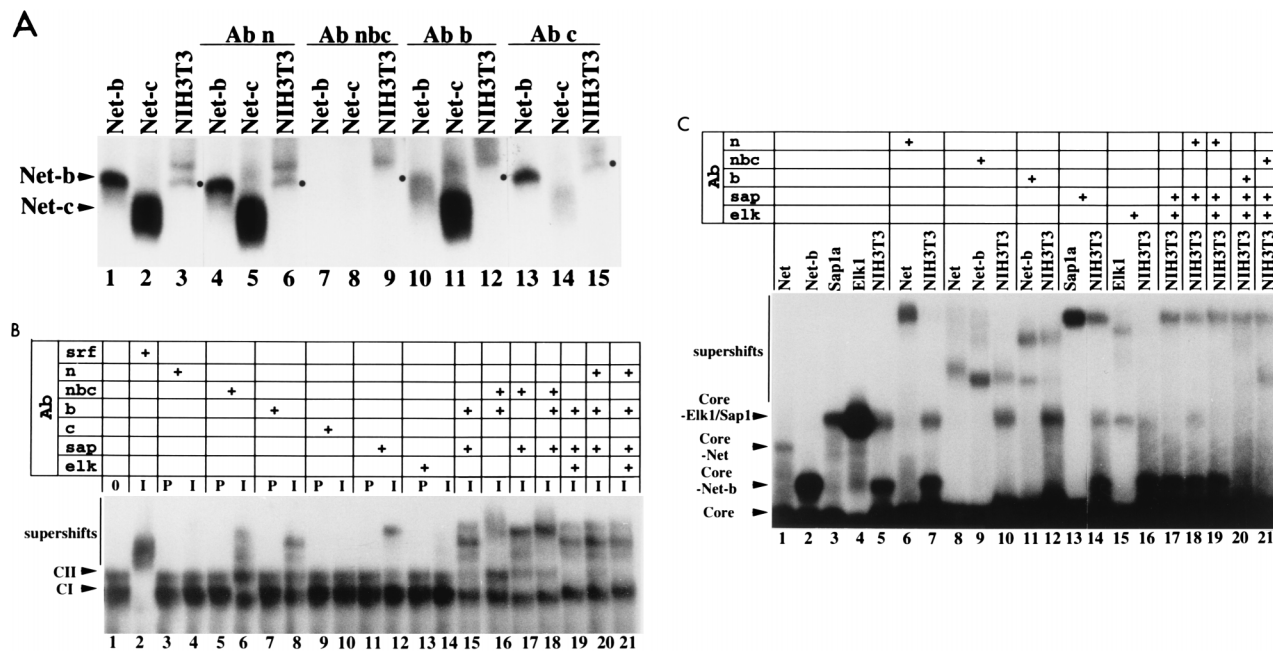
FIG. 7. Supershifts of TCFs from NIH 3T3 cells. (A) NIH 3T3 nuclear extracts and in vitro-synthesized Net-b and Net-c were incubated with the PEA3* probe and analyzed by mobility shift assays in the absence of specific antibodies or after incubation with Ab n, Ab nbc, Ab b, and Ab c. The Net-b and Net-c complexes are indicated by arrowheads, and the position of the specific complex formed with cell extracts is indicated by a dot. The incubation mixes included 20% glycerol, 1 μg of poly(dI-dC) and 250 ng of salmon sperm DNA, and the gels contained 2.5% glycerol. (B) NIH 3T3 nuclear extracts (30 μg) were incubated with the SRE probe and preimmune sera (P) or immune sera (I,) that interact with SRF (Ab srf), Net (Ab n), Net plus Net-b plus Net-c (Ab nbc) Net-b (Ab b), Net-c (Ab c), and antibodies against Sap1 (Ab sap), Elk1 (Ab elk), Net-b plus Sap1 (Ab b), Net plus Net-b plus Net-c (Ab nbc + Ab b), Net plus Net-b plus Net-c plus Sap1 (Ab nbc + Ab sap), Net plus Net-b plus Net-c plus Sap1 (Ab nbc + Ab b + Ab sap), Net-b plus Sap1 plus Elk1 (Ab b + Ab sap + Ab elk), Net plus Net-b plus Sap1 (Ab n + Ab b + Ab sap), and Net plus Net-b plus Sap1 plus Elk1 (Ab n + Ab b + Ab sap + Ab elk). CI and CII (indicated by arrowheads) are specific bands, and supershifts altered mobility complexes displaced by antibodies. The incubations included 250 ng of salmon sperm DNA and 4% Ficoll [without poly(dI-dC) and glycerol)], and the gels did not contain glycerol. (C) Band shifts with added core SRF (amino acids 132 to 222, all lanes), in vitro-translated Net, Net-b, Sap1a, Elk1, and 30 μg of NIH 3T3 nuclear extracts. The reaction mixtures contained the following immune sera: Ab n, Ab nbc, Ab b, Ab sap, and Ab elk. Arrowheads point to the indicated complexes, and the line indicates the region of the gel with supershifted complexes. The incubations included 250 ng of salmon sperm DNA and 4% Ficoll [without poly(dI-dC) and glycerol], and the gels did not contain glycerol.

iments as well as Western blots (see above) whereas Net-c is not detected by either method.

In experiments with the SRE probe, the effects of the anti-TCF sera (Fig. 7B, lanes I) were compared with the corresponding preimmune sera (lanes P). In the absence of antibodies, two complexes were observed, CI and CII (lane 1). CI migrated at the same level as SRF and SRF plus Net-b, and CII migrated at the same level as SRF plus Sap1a and SRF plus Elk1 (compare with Fig. 5A and 6B, using in vitro-synthesized proteins). Ab srf displaced both the CI and CII complexes, showing that they all contain SRF (Fig. 7B, compare lanes 1 and 2). Ab n had little effect on either complex (lanes 3 and 4, with the preimmune and immune serum, respectively). Both Ab nbc and Ab b decreased the intensity of the CI band by at least 50% (lanes 5 to 8). Ab c has no effect (lanes 9 and 10), consistent with the absence of detectable amounts of Net-c protein in these cells. Ab sap displaced more than 50% of CII (lanes 11 and 12), whereas Ab elk decreased the CII band to a smaller but detectable extent in different experiments (lanes 13 and 14 and data not shown). These results suggest that CI is composed of free SRF and SRF plus Net-b whereas CII has both SRF plus Sap1 and SRF plus Elk1. This was confirmed with combinations of antibodies. Ab sap with various combinations of Net-b-targeted antibodies decreased the intensities of both the CI and CII bands (lanes 15, 17, and 20). This was not merely the effect of mixing two antibodies, since, as expected, Ab nbc plus Ab b only decreased CI and the pattern of supershifted bands was altered (lane 16). Combining antibod-

ies against the three different TCFs (Net-b, Sap1, and Elk1) decreased CI and abolished CII (lanes 19 and 21), whereas the mere combination of three antibodies without Elk1 antibodies was not sufficient to completely remove CII (lane 20).

TC formation was also studied with exogenous core SRF, which forms smaller TCs that can be resolved more easily (Fig. 7C). The mobilities of the core TCs were determined with in vitro-translated proteins (Fig. 7C, lanes 1 to 4). NIH 3T3 cell extracts gave bands of higher mobility that comigrated with Net-b–core and bands of lower mobility running at the level of SAP1-core and Elk1-core complexes (lane 5). There was a trace amount of an intermediary band at the level of Net-core. Antibodies were used to confirm their composition. Ab n supershifted the control Net complex and had little overall effect on the complexes from cell extracts (lanes 6 and 7). However, a faint Net supershift was observed, especially upon longer exposure of the autoradiograms (data not shown), indicating that there is a small amount of Net. Ab nbc displaced both the Net and Net-b complexes, forming major supershifted complexes with different mobilities (lanes 8 and 9). With cell extracts, Ab nbc eliminated the faster-migrating complex (core–Net-b, lane 10) and formed the expected supershifted Net-b band (lanes 9 and 10). Ab b also specifically eliminated the same complex and formed the expected supershifted Net-b bands (lanes 11 and 12). Ab sap specifically decreased the intensity of the lower-mobility complex by over 50% and formed supershifted complexes that comigrated with Sap1a (lanes 13 and 14). Ab elk specifically decreased the intensity of

FIG. 8. Composition of TCs from EGF-stimulated NIH 3T3 cells and LPS-differentiated 70Z/3 cells. (A) Nuclear extracts (30 μg) from NIH 3T3 that were serum starved (lanes 0) or stimulated with EGF for 30 min (lanes 30′) or 90 min (lanes 90′) were incubated with the SRE probe. Incubations were performed without antibodies or with Ab srf, Ab n, Ab nbc, Ab b, Ab sap, Ab elk, Ab b plus Ab sap, Ab b plus Ab sap plus Ab elk, and Ab n plus Ab b plus Ab sap. Arrowheads indicate the bands CI and CII, and the line indicates supershifted complexes. The incubations included 250 ng of salmon sperm DNA and 4% Ficoll [without poly(dI-dC) and glycerol], and the gels did not contain glycerol. (B) Band shifts with added core SRF (amino acids 132 to 222, all lanes) and 30 μg of nuclear extracts from NIH 3T3 cells that were serum starved (lanes 0) or incubated with EGF for 30 min (lanes 30′) or 90 min (lanes 90′). The reaction mixtures contained the following immune sera: Ab n, Ab nbc, Ab b, Ab sap, Ab elk, and Ab nbc plus Ab sap plus Ab elk. Arrowheads point to the indicated complexes, and the line indicates supershifted complexes. The incubations included 250 ng of salmon sperm DNA and 4% Ficoll [without poly(dI-dC) and glycerol], and the gels did not contain glycerol. (C) The band shifts contained core SRF (amino acids 132 to 222, all lanes) and nuclear extracts (30 μg) from either 70Z/3 or NIH 3T3 cells. The 70Z/3 cells were either unstimulated (0 h) or incubated with LPS for 30 min (0.5 h) or 240 min (4 h), and the NIH 3T3 cells were either serum starved (0 h) or incubated with EGF for either 30 min (0.5 h) or 90 min (1.5 h). Incubations either lacked antibodies or contained Ab n, Ab nbc, Ab sap, or Ab elk. The arrows point to the indicated complexes, and the line indicates the supershifted bands. The incubations included 250 ng of salmon sperm DNA and 4% Ficoll [without poly(dI-dC) and glycerol], and the gels did not contain glycerol.

the same band, showing that it also contains Elk1 complexes (lane 15). Ab elk displaced virtually all of the in vitro complex without forming an equivalent amount of supershifted complex (compare lanes 15 and 4), indicating that Ab elk dissociates the complex. Combinations of antibodies gave the expected results. Ab sap plus Ab elk specifically and completely eliminated the upper complex (lane 17), whereas Ab sap with a non-Elk1 antibody (Ab n) did not (lane 18). Combining Ab sap and Ab elk with Ab nbc or Ab b eliminated both complexes (lanes 20 and 21). We estimate by scanning these and other autoradiograms that TCs formed with extracts from continuously growing NIH 3T3 cells contain about 60% Net-b, 25% Sap1, and 15% Elk1. We estimate that they account for at least 90% of the TCFs that can form stable complexes under our conditions.

TC composition in NIH 3T3 cells that were serum starved and stimulated with EGF was studied. EGF increased the amount of both the CI and CII complexes after 30 and 90 min of treatment (Fig. 8A, lanes 1 to 3; Fig. 5A). Ab srf supershifted both CI and CII (Fig. 8A, lanes 4 to 6). Ab n had little overall effect on the complexes but produced a detectable and reproducible supershift (lanes 7 to 9). Individually, Ab nbc and

Ab b decreased the intensity of CI (lanes 10 to 15), and Ab sap and Ab elk decreased the intensity of CII (lanes 16 to 21). Ab sap with Ab b decreased the intensities of both CI and CII (lanes 22 to 24). Adding Ab elk eliminated CII (lanes 25 to 27), whereas adding Ab n did not (lanes 28 to 30). With added core SRF, three TCs were detected, corresponding to core with Net-b, Net, and a mixture of Elk1 and Sap1. Ab n supershifted the faint Net complex (Fig. 8B, lanes 4 to 6, compare especially lanes 5 and 6 with lanes 2 and 3). Ab nbc and Ab b displaced the Net-b complex (lanes 7 to 12), Ab sap and Ab elk affected the Sap1-plus-Elk1 band (lanes 13 to 15 and 16 to 18, respectively), and the combination of antibodies against all of the TCFs (Ab nbc plus Ab sap plus Ab elk) displaced all of the ternary complexes (lanes 19 to 21). These results show that in serum-starved and EGF-stimulated NIH 3T3 cell extracts, the TCs contain Net-b > Elk1 ≥ Sap1 > Net (about 60:20:15:5). EGF stimulation for 30 and 90 min led to similar increases in the amounts of all three factors. The relative levels of the TCFs were not strikingly different from those in continuously growing NIH 3T3 cells.

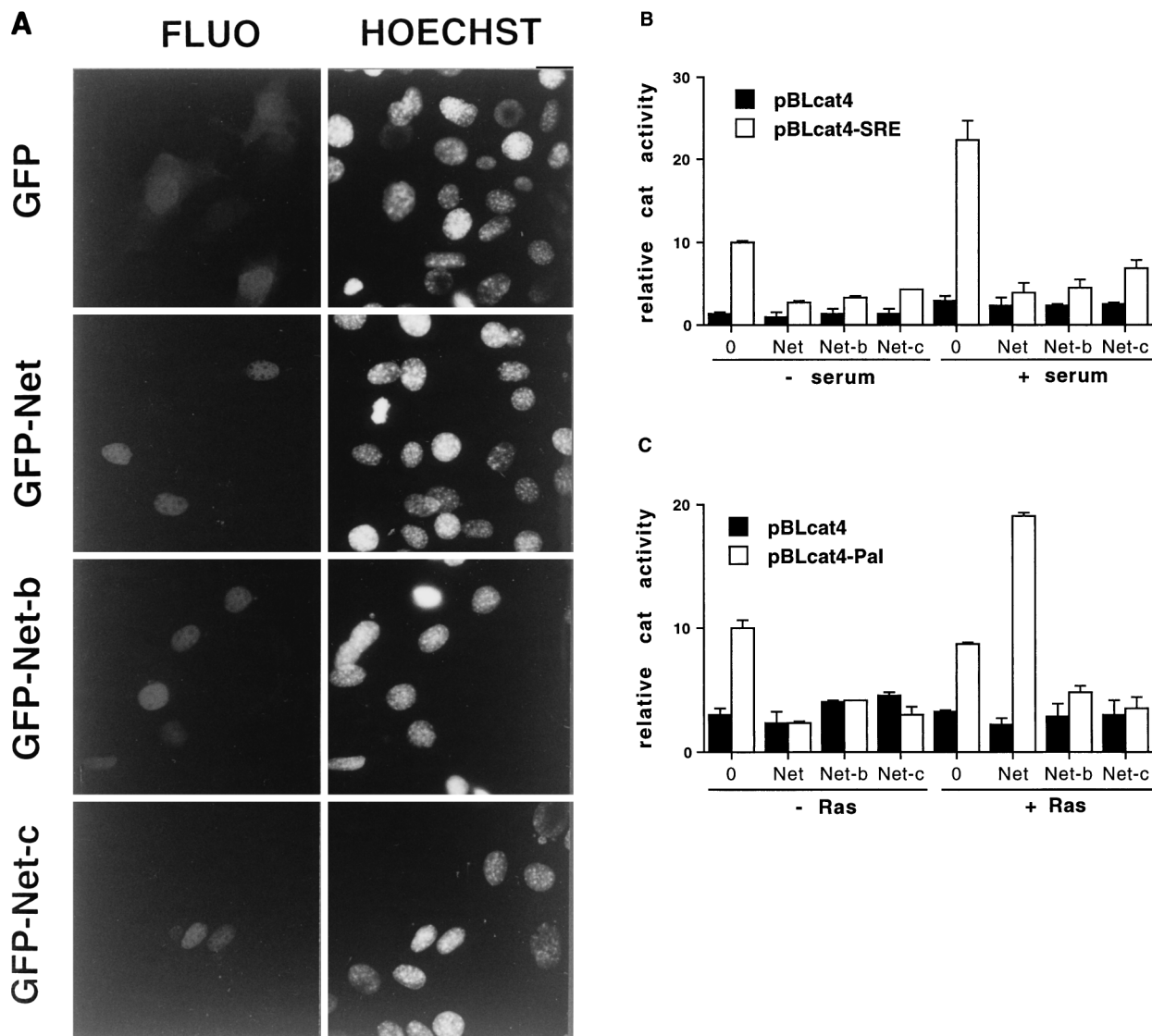The relative levels of the TCFs in 70Z/3 cells before and

FIG. 9. Cellular localization (A) and effects of serum (B) and Ras (C) on the transcriptional activities of Net, Net-b, and Net-c. (A) NIH 3T3 cells were transfected with expression vector encoding either GFP (pE.GFP.C1), GFP-Net (pGFP.Net), GFP-Net-b (pGFP.Net-b), or GFP-Net-c (pGFP.Net-c). They were examined under a fluorescence microscope with either an FITC filter for green fluorescence from the GFP fusion proteins (left panels) or a UV filter for Hoechst nuclear staining (right panels). (B and C) The transfections contained 2.5 μg of pTL2-based vectors that express Net, Net-b, or Net-c; 3 μg of reporters with the wild-type SRE (B, pBLCAT4-SRE) or eight palindromic *ets* motifs (C, pBLCAT4-Pal) or lacking a specific response element (B and C, pBLCAT4); 3 μg of pSG5-lacZ to control for transfection efficiency; and pEMBL to fill up to 20 μg. (B) NIH 3T3 cells were transfected and incubated with (+) or without (−) serum for 24 h. (C) The transfection mixtures contained 2.5 μg of either an expression vector for mutated Ha-Ras (pRCBx2, +Ras) or a control vector (pΔRCBx2, −Ras).

after treatment with LPS were also studied (Fig. 8C). Core SRF formed three TC bands that comigrated with the characterized complexes from NIH 3T3 cells (compare lanes 1 to 3 with lanes 16 to 18). The assignment of the bands was confirmed with antibodies (Ab n [lanes 4 to 6], Ab nbc [lanes 7 to 9], Ab sap [lanes 10 to 12], and Ab elk [lanes 13 to 15]). The relative amounts of the TCFs in the TCs, estimated from the relative intensities of the bands and from the effects of Ab sap and Ab elk (lanes 10 to 15), were SAP1 > Net-b > Elk1 > Net (quantitated to about 55:30:10:5). The absolute and relative amounts of the complexes did not change substantially after LPS treatment (less than twofold [Fig. 2B, 3B, 3C, and 5B]). These results show that 70Z/3 pre-B cells express less Net-b relative to Sap1 than do NIH 3T3 fibroblasts.

Net-b is nuclear and is an inhibitor of transcription. Net-b and Net-c lack the Ras-inducible C domain of Net yet retain the essential helix-loop-helix motif of the Net inhibitor domain NID (10, 34). Net-b and Net-c were shown to be nuclear proteins, using GFP-Net fusion proteins expressed in NIH 3T3 cells. Unfused GFP gave a diffuse fluorescence throughout the cell (Fig. 9A, compare the fluorescence with the Hoechst nuclear staining), whereas GFP–Net, GFP–Net-b, and GFP–Net-c gave bright nuclear fluorescence. The three unfused Net proteins were also found to be nuclear when they were expressed in both COS and NIH 3T3 cells and detected by immunocytochemistry with specific antibodies (data not shown). The transcriptional activities of Net-b and Net-c were tested in transfection assays in NIH 3T3 cells with SRE-CAT

and *ets* motif Pal-CAT reporters (10). As reported previously, Net expression inhibited SRE-driven CAT expression, under both low-serum conditions and after induction of SRE activity with high serum levels (Fig. 9B). Net-b and Net-c also inhibited transcription under both conditions. We have shown previously that Net inhibits the *ets* motif reporter and Ras switches Net to a positive activator, mainly through effects on the Ras-inducible activation domain, the C domain (10, 34) (Fig. 9C). Net-b and Net-c inhibited transcription from the *ets* motif reporter in both the absence and presence of the Ras signal (Fig. 9C), as expected from the lack of the C domain and the presence of the helix-loop-helix motif. It is unlikely that inhibition results from squelching of general transcription factors, since Net-b and Net-c lack the C activation domain, or that it results from an indirect effect from the cytoplasm, since they are localized in the nucleus. In conclusion, Net-b and Net-c behave as constitutive inhibitors of transcription.

DISCUSSION

Complexity of the TCF family. We have determined the structure of the *net* gene and shown that it encodes a novel alternative splice product, Net-b. The mouse *net* gene has certain features in common with the recently published *elk1* gene (13). Most of the Ets domain (about 70 amino acids) is encoded by the first coding exon. The middle (almost 300 amino acids) of Net and Elk1 is encoded by one complex or two exons, respectively. The C domain and C terminus are formed from two exons, the first of which is quite short, coding for about 40 amino acids.

net-b RNA was detected by both RNase mapping and splice junction-specific PCR. It is found in a wide range of tissues. Its levels relative to *net* vary, most notably in mouse heart and liver and the pre-B-cell line 70Z/3. The protein was detected in several cell lines with two antibodies raised against distinct epitopes. Two techniques were used, Western blotting and supershifting of proteins bound to specific DNA probes. The supershifts show that it is one of the major TCFs that complexes to SRF and the c-*fos* SRE. In continuously growing NIH 3T3 cells, it is more abundant than Sap1, which was previously thought to be the major TCF in these cells (22).

We also detected a second potential splice product, Net-c. However, *net-c* mRNA was detected only in NIH 3T3 and rat 3T3 cells, and the protein was not detectable with our antibodies. *net-c* might be expressed at very low levels and/or in a very restricted manner. The same splice junctions are used for other RNAs, suggesting that *net-c* RNA may be a low-efficiency by-product of splicing with no functional consequences. A cryptic splice product has also been described for the *elk1* gene (13). It remains to be seen if *net-c* RNA and Net-c protein are expressed at appreciable levels in other cells.

Net-b has both similarities to and differences from the other TCFs. Net-b, like Sap1b, lacks the Ras-inducible C domain that is found in Net, Sap1a, and Elk. It contains the helix-loop-helix that mediates repression by Net (34). As predicted, Net-b is an inhibitor of transcription in NIH 3T3 cells, both with and without a Ras signal. Net is converted from a repressor to an activator by Ras. In the same cells, without Ras, Sap1a is inactive whereas Elk1 stimulates. Ras activates Sap1a and to a small extent Elk1 (10, 34). Sap1b has not been characterized, but it is predicted to be a passive competitive inhibitor of the other factors. The interesting and unresolved question is why are there so many factors to mediate the transcription regulation of the *fos* promoter through the SRE.

Role of negative factors in the regulation of the *fos* promoter. Genomic footprinting of the c-*fos* promoter around the

SRE shows that it is continuously occupied by proteins in vivo, suggesting that TC formation is not required for growth factor induction (18, 30). However, the composition of the complex may vary. The in vivo footprint is identical to the TCF-SRE pattern generated in vitro, suggesting that it does not detect differences in composition. TC formation is a dynamic process in vitro, suggesting that there could be exchange in vivo and that the components of the complex may vary under different conditions (reviewed in reference 53). We have studied the composition of TCs formed in vitro with cell extracts, which may reflect the composition of TCs in vivo.

Extracts from continuously cycling as well as serum-with-drawn NIH 3T3 fibroblasts form TCs that contain predominantly Net-b and less Sap1 and Elk1. The *fos* promoter is inactive under these conditions (12), suggesting that it is repressed by factors such as Net-b. We have found that down-regulation of Net proteins with *net* antisense RNA stimulates SRE activity in actively growing and serum-starved cells (10, 11a), as would be expected if Net-b actively represses the promoter. A role for negative factors in keeping a promoter inactive is suggested by the work of Price et al. (38). They found that UV activation of the c-*fos* promoter through the TCFs requires both the ERK and p38 kinase pathways, suggesting that the promoter will respond only to a certain threshold level of activation. The promoter may be dampened against random low-level activating signals, and this could be achieved by negative factors such as Net-b that keep it inactive until there is a strong positive signal.

Activation with EGF increases the amount of all of the complexes that form on the SRE, including those that contain just SRF. SRF is known to respond to signalling cascades independently of the TCFs (19, 20, 28, 41). A somewhat surprising observation is that EGF stimulates negative as well as positive TCFs. We have shown previously that *net* antisense increases SRE activity in cells that have been starved of serum as well as stimulated by serum and that the effect of antisense is greater in serum-stimulated cells than in serum-starved cells (10). We propose that the balance between positive and negative factors is necessary for both the rise and the subsequent rapid fall in the activity of the SRE. Activation is probably mediated by phosphorylation of TCFs such as Sap1 and Elk1. The increase in the level of Net-b would contribute to the decrease in SRE activity.

A variety of observations suggest that SREs could be involved in the regulation of development (5, 14, 47, 51). Net is highly expressed in pre-B cells but not in mature B cells (33). To explore the potential role of Net-b in B-cell development, we studied the pre-B cell line, 70Z/3, which can be induced to differentiate with LPS. LPS is known to stimulate SRE activity (24), Fos-Jun DNA binding activity (43), and p38 MAP kinase (16, 17). We found that LPS induction of 70Z/3 pre-B-cell differentiation increases TC-forming activity to a small extent. The complexes contain SAP1 with a smaller amount of Net-b and very little Elk1. In contrast to 70Z/3, there is more Net-b than SAP1 in NIH 3T3 cells. The composition of TCs is different in a number of cell types, including epithelial cells (HeLa [references 23 and 37 and data not shown], macrophages [BAC-1] [22], and astrocytomas [A431] [49]). These results suggest that the TCFs play cell-type-specific roles. There are at least five TCFs, including the new factor, Net-b, that we describe in this report. Elucidating the roles of the plethora of TCFs should provide important insights into how signal transduction through the Ras signalling network is resolved into specific physiological responses.

ACKNOWLEDGMENTS

REFERENCES

1. **Beitel, G. J., S. Tuck, I. Greenwald, and H. R. Horvitz.** 1995. The Caenorhabditis elegans gene lin-1 encodes an ETS-domain protein and defines a branch of the vulval induction pathway. Genes Dev. **9:**3149–3162.
2. **Bradford, A. P., K. E. Conrad, C. Wasylyk, B. Wasylyk, and A. Gutierrez-Hartmann.** 1995. Functional interaction of c-Ets-1 and GHF-1/Pit-1 mediates Ras activation of pituitary-specific gene expression: mapping of the essential c-Ets-1 domain. Mol. Cell. Biol. **15:**2849–2857.
3. **Brunner, D., K. Ducker, N. Oellers, E. Hafen, H. Scholz, and C. Klambt.** 1994. The ETS domain protein-P2 is a target of MAP kinase in the sevenless signal transduction pathway. Nature **370:**386–389.
4. **Coffer, P., M. de Jonge, A. Mettouchi, B. Binetruy, J. Ghysdael, and W. Kruijer.** 1994. junB promoter regulation: Ras mediated transactivation by c-Ets-1 and c-Ets-2. Oncogene **9:**911–921.
5. **Croissant, J. D., J.-H. Kim, G. Eichele, L. Goering, J. Lough, R. Prywes, and R. J. Schwartz.** 1996. Avian serum response factor expression restricted primarily to muscle cell lineages is required for a-actin gene transcription. Dev. Biol. **177:**250–264.
6. **Downward, J.** 1995. KSR: a novel player in the RAS pathway. Cell **83:**831–834.
7. **Galang, C. K., C. J. Der, and C. A. Hauser.** 1994. Oncogenic Ras can induce transcriptional activation through a variety of promoter elements, including tandem c-Ets-2 binding sites. Oncogene **9:**2913–2921.
8. **Gille, H., M. Kortenjann, O. Thomae, C. Moomaw, C. Slaughter, M. H. Cobb, and P. E. Shaw.** 1995. ERK phosphorylation potentiates Elk-1-mediated ternary complex formation and transactivation. EMBO J. **14:**951–962.
9. **Gille, H. G., A. D. Sharrocks, and P. E. Shaw.** 1992. Phosphorylation of transcription factor p62TCF by MAP kinase stimulates ternary complex formation at the c-fos promotor. Nature **358:**414–417.
10. **Giovane, A., A. Pintzas, S. M. Maira, P. Sobieszczuk, and B. Wasylyk.** 1994. Net, a new ets transcription factor that is activated by Ras. Genes Dev. **8:**1502–1513.
11. **Giovane, A., P. Sobieszczuk, C. Mignon, M. G. Mattei, and B. Wasylyk.** 1995. Locations of the ets subfamily members net, elk1, and sap1 (ELK3, ELK1, and ELK4) on three homologous regions of the mouse and human genomes. Genomics **29:**769–772.
11a.**Giovane, A., and B. Wasylyk.** Unpublished results.
12. **Greenberg, M. E., and E. B. Ziff.** 1984. Stimulation of 3T3 cells induces transcription of the c-fos proto-oncogene. Nature **311:**433–438.
13. **Grevin, D., S. Ung, F. Denhez, M. Dehem, B. Quatannens, A. Begue, D. Stehelin, and P. Martin.** 1996. Structure and organization of the mouse elk1 gene. Gene **174:**185–188.
14. **Guillemin, K., J. Groppe, K. Ducker, R. Treisman, E. Hafen, M. Affolter, and M. A. Krasnow.** 1996. The pruned gene encodes the Drosophila serum response factor and regulates cytoplasmic outgrowth during terminal branching of the tracheal system. Development **122:**1353–1362.
15. **Gum, R., E. Lengyel, J. Juarez, J. H. Chen, H. Sato, M. Seiki, and D. Boyd.** 1996. Stimulation of 92-kDa gelatinase B promoter activity by ras is mitogen-activated protein kinase kinase 1-independent and requires multiple transcription factor binding sites including closely spaced PEA3/ets and AP-1 sequences. J. Biol. Chem. **271:**10672–10680.
16. **Han, J., J. D. Lee, L. Bibbs, and R. J. Ulevitch.** 1994. A MAP kinase targeted by endotoxin and hyperosmolarity in mammalian cells. Science **265:**808–811.
17. **Han, J., J. D. Lee, P. S. Tobias, and R. J. Ulevitch.** 1993. Endotoxin induces rapid protein tyrosine phosphorylation in 70Z/3 cells expressing CD14. J. Biol. Chem. **268:**25009–25014.
18. **Herrera, R. E., P. E. Shaw, and A. Nordheim.** 1989. Occupation of the c-fos serum response element in vivo by a multi-protein complex is unaltered by growth factor induction. Nature **340:**68–70.
19. **Hill, C. S., J. Wynne, and R. Treisman.** 1994. Serum-regulated transcription by serum response factor (SRF): a novel role for the DNA binding domain. EMBO J. **13:**5421–5432.
20. **Hill, C. S., J. Wynne, and R. Treisman.** 1995. The Rho family GTPases RhoA, Rac1, and CDC42Hs regulate transcriptional activation by SRF. Cell **81:**1159–1170.
21. **Hipskind, R. A., M. Baccarini, and A. Nordheim.** 1994. Transient activation

22. of RAF-1, MEK, and ERK2 coincides kinetically with ternary complex factor phosphorylation and immediate-early gene promoter activity in vivo. Mol. Cell. Biol. **14:**6219–6231.
22. **Hipskind, R. A., D. Buscher, A. Nordheim, and M. Baccarini.** 1994. Ras/MAP kinase-dependent and -independent signaling pathways target distinct ternary complex factors. Genes Dev. **8:**1803–1816.
23. **Hipskind, R. A., V. N. Rao, C. G. Mueller, E. S. Reddy, and A. Nordheim.** 1991. Ets-related protein Elk-1 is homologous to the c-fos regulatory factor p62TCF. Nature **354:**531–534.
24. **Janknecht, R., M. A. Cahill, and A. Nordheim.** 1995. Signal integration at the c-fos promoter. Carcinogenesis **16:**443–450.
25. **Janknecht, R., W. H. Ernst, and A. Nordheim.** 1995. SAP1a is a nuclear target of signaling cascades involving ERKs. Oncogene **10:**1209–1216.
26. **Janknecht, R., D. Monte, J. L. Baert, and Y. de Launoit.** 1996. The ETS-related transcription factor ERM is a nuclear target of signaling cascades involving MAPK and PKA. Oncogene **13:**1745–1754.
27. **Janknecht, R., and A. Nordheim.** 1992. Elk-1 protein domains required for direct and SRF-assisted DNA-binding. Nucleic Acids Res. **20:**3317–3324.
28. **Johansen, F.-E., and R. Prywes.** 1994. Two pathways for serum regulation of the c-fos serum response element require specific sequence elements and a minimal domain of serum response factor. Mol. Cell. Biol. **14:**5920–5928.
29. **Kiaris, H., and D. A. Spandidos.** 1995. Mutations of ras genes in human tumours. Int. J. Oncol. **7:**413–421.
30. **Konig, H., H. Ponta, U. Rahmsdorf, M. Buscher, A. Schonthal, H. J. Rahmsdorf, and P. Herrlich.** 1989. Autoregulation of fos: the dyad symmetry element as the major target of repression. EMBO J. **8:**2559–2566.
31. **Lai, Z. C., and G. M. Rubin.** 1992. Negative control of photoreceptor development in Drosophila by the product of the yan gene, an ETS domain protein. Cell **70:**609–620.
32. **Langer, S. J., D. M. Bortner, M. F. Roussel, C. J. Sherr, and M. C. Ostrowski.** 1992. Mitogenic signaling by colony-stimulating factor 1 and ras is suppressed by the ets-2 DNA-binding domain and restored by myc overexpression. Mol. Cell. Biol. **12:**5355–5362.
33. **Lopez, M., P. Oettgen, Y. Akbarali, U. Dendorfer, and T. A. Libermann.** 1994. ERP, a new member of the ets transcription factor/oncoprotein family: cloning, characterization, and differential expression during B-lymphocyte development. Mol. Cell. Biol. **14:**3292–3309.
34. **Maira, S.-M., J.-M. Wurtz, and B. Wasylyk.** 1996. Net (ERP/SAP2), one of the Ras inducible TCFs, has a novel inhibitory domain with resemblance to the helix-loop-helix motif. EMBO J. **15:**5849–5865.
35. **Marais, R., J. Wynne, and R. Treisman.** 1993. The SRF accessory protein Elk-1 contains a growth factor-regulated transcriptional activation domain. Cell **73:**381–393.
36. **O'Neill, E. M., I. Rebay, R. Tjian, and G. M. Rubin.** 1994. The activities of two Ets-related transcription factors required for Drosophila eye development are modulated by the Ras/MAPK pathway. Cell **78:**137–147.
37. **Pingoud, V., R. Zinck, R. A. Hipskind, R. Janknecht, and A. Nordheim.** 1994. Heterogeneity of ternary complex factors in HeLa cell nuclear extracts. J. Biol. Chem. **269:**23310–23317.
38. **Price, M. A., F. H. Cruzalegui, and R. Treisman.** 1996. The p38 and ERK MAP kinase pathways cooperate to activate ternary complex factors and c-fos transcription in response to UV light. EMBO J. **15:**6552–6563.
39. **Price, M. A., A. E. Rogers, and R. Treisman.** 1995. Comparative analysis of the ternary complex factors Elk-1, SAP-1a and SAP-2 (ERP/NET). EMBO J. **14:**2589–2601.
40. **Rao, V. N., K. Huebner, M. Isobe, A. ar-Rushdi, C. M. Croce, and E. S. Reddy.** 1989. elk, tissue-specific ets-related genes on chromosomes X and 14 near translocation breakpoints. Science **244:**66–70.
41. **Rivera, V. M., C. K. Miranti, R. P. Misra, D. D. Ginty, R.-H. Chen, J. Blenis, and M. E. Greenberg.** 1993. A growth factor-induced kinase phosphorylates the serum response factor at a site that regulates its DNA-binding activity. Mol. Cell. Biol. **13:**6260–6273.
42. **Sadowski, H. B., and M. Z. Gilman.** 1993. Cell-free activation of a DNA-binding protein by epidermal growth factor. Nature **362:**79–83.
43. **Schanke, J. T., A. Marcuzzi, R. P. Podzorski, and B. Van Ness.** 1994. An AP1 binding site upstream of the kappa immunoglobulin intron enhancer binds inducible factors and contributes to expression. Nucleic Acids Res. **22:**5425–5432.
44. **Sgouras, D. N., M. A. Athanasiou, G. J. Beal, R. J. Fisher, D. G. Blair, and G. J. Mavrothalassitis.** 1995. ERF: an ETS domain protein with strong transcriptional repressor activity, can suppress ets-associated tumorigenesis and is regulated by phosphorylation during cell cycle and mitogenic stimulation. EMBO J. **14:**4781–4793.
45. **Sharp, P. A.** 1994. Split genes and RNA splicing. Cell **77:**805–815.
46. **Shaw, P. E., S. Frasch, and A. Nordheim.** 1989. Repression of c-fos transcription is mediated through p67SRF bound to the SRE. EMBO J. **8:**2567–2574.
47. **Taylor, M., R. Treisman, N. Garrett, and T. Mohun.** 1989. Muscle-specific (CArG) and serum-responsive (SRE) promoter elements are functionally interchangeable in Xenopus embryos and mouse fibroblasts. Development **106:**67–78.
48. **Tei, H., I. Nihonmatsu, T. Yokokura, R. Ueda, Y. Sano, T. Okuda, K. Sato,

K. Hirata, S. C. Fujita, and D. Yamamoto. 1992. pokkuri, a Drosophila gene encoding an E-26-specific (Ets) domain protein, prevents overproduction of the R7 photoreceptor. Proc. Natl. Acad. Sci. USA **89:**6856–6860.

49. **Thompson, M. J., M. W. Roe, R. K. Malik, and P. J. Blackshear.** 1994. Insulin and other growth factors induce binding of the ternary complex and a novel protein complex to the c-fos serum response element. J. Biol. Chem. **269:**21127–21135.

50. **Treisman, R.** 1996. Regulation of transcription by MAP kinase cascades. Curr. Opin. Cell Biol. **8:**205–215.

51. **Tuil, D., N. Clergue, D. Montarras, C. Pinset, A. Kahn, and F. Phan-Dinh-Tuy.** 1990. CC Ar GG boxes, cis-acting elements with a dual specificity. Muscle-specific transcriptional activation and serum responsiveness. J. Mol. Biol. **213:**677–686.

52. **Wasylyk, B., S. L. Hahn, and A. Giovane.** 1993. The Ets family of transcrip-

tion factors. Eur. J. Biochem. **211:**7–18. (Erratum, **215:**907, 1993.)

53. **Wasylyk, B., and A. Nordheim.** 1997. Ets transcription factors: partners in the integration of signal responses, p. 251–284. *In* A. G. Papavassiliou (ed.), Transcription factors in eucaryotes. R. G. Landes Co., Georgetown, Tex.

54. **Wasylyk, C., A. P. Bradford, A. Gutierrez-Hartmann, and B. Wasylyk.** 1997. Conserved mechanisms of Ras regulation of evolutionary related transcription factors, Ets1 and Pointed P2. Oncogene **14:**899–913.

55. **Wasylyk, C., S. M. Maira, P. Sobieszczuk, and B. Wasylyk.** 1994. Reversion of Ras transformed cells by Ets transdominant mutants. Oncogene **9:**3665–3673.

56. **Zinck, R., R. A. Hipskind, V. Pingoud, and A. Nordheim.** 1993. c-fos transcriptional activation and repression correlate temporally with the phosphorylation status of TCF. EMBO J. **12:**2377–2387.